Numerical Study for the Effect of the Contraction Ratio on the Cavitating Venturi Internal Flow Pattern

Gong Hee Lee [a*], June Ho Bae [a]
[a]*Regulatory Assessment Department, Korea Institute of Nuclear Safety, Daejeon, 34142, Korea*
[*]*Corresponding author: ghlee@kins.re.kr*

1. Introduction

Domestic nuclear power plant operators have conducted in-service testing (IST) to verify the safety functions of safety-related pumps and valves, and to monitor the degree of vulnerability over time during reactor operation [1]. The auxiliary feedwater system is one of the representative IST-related system and a cavitating venturi is installed to prevent cavitation due to pump runout and minimize other adverse effects resulting from the supply of excessive auxiliary feedwater flows [2]. Rapid flow acceleration and accompanying pressure drop may cause cavitation near the straight throat and diffusion section of venturi, which may result in degradation and structural damage [1].

The main geometrical parameters that affect the cavitation flow occurring in a cavitating venturi include the inclination angle of the contraction section, the contraction ratio for the straight throat section, and the inclination angle of the diffusion section (refer to Fig. 1). Among these geometrical parameters, the effect of contraction angle and diffusion angle on the cavitation flow patterns were closely examined in the author's previous study [3, 4]. In this study, simulation of cavitation flow inside a cavitating venturi was conducted with commercial CFD software, ANSYS CFX R19.1 to investigate the internal flow pattern depending on the contraction ratio for the straight throat section of the cavitating venturi.

2. Analysis Model

Fig. 1 shows a schematic diagram for the analysis model. A cavitating venturi consists of an upstream, contraction, throat, diffusion and downstream section [1]. Geometrical specification for the analysis model was summarized in Table I. Except throat diameter (d) and the corresponding contraction ratio (γ), the magnitudes of other geometrical parameters were fixed in this study.

Fig. 1. Schematic diagram for the analysis model.

A pressure transducer with an accuracy of ± 0.4% recorded inlet pressure [5]. Outlet pressure remained constant and was equal to the atmospheric pressure [5]. The flow rate was monitored using the flow meter with an accuracy of ± 3% [5]. The working fluid was 20°C water.

Table I: Geometrical specification for the analysis model.

Parameters	Unit	Magnitudes
Inlet/Outlet diameter (D)	mm	12.7
Throat diameter (d)	mm	**1.91, 3.18, 4.45**
Contraction ratio ($\gamma=d/D$)	-	**0.15, 0.25, 0.35**
Throat length (L)	mm	20.0
Contraction angle (α)	deg.	38.0
Diffusion angle (β)	deg.	10.0

In case of contraction ratio (γ), three different magnitudes, i.e. 0.15, 0.25 and 0.35, were chosen.

3. Numerical Modeling

The validity of the numerical modeling applied in this study can be found in the author's previous study [1].

3.1 Numerical Method

It was assumed that the flow inside a cavitating venturi was steady, incompressible, turbulent and multiphase flow. High resolution scheme with the quasi-second order accuracy was used for the convection-terms-of-momentum and -turbulence equations. For Interphase Transfer Model setting, mixture model was chosen [1]. Rayleigh-Plesset cavitation model was used to simulate the cavitation flow and saturation pressure set to 2,338 Pa [1]. The solution was considered to be 'converged' when the residuals of variables were below 10^{-6} and the variations of the target variables were small [1].

3.2 Turbulence Model

Shear Stress Transport (SST) k-ω model, which is one of Reynolds-averaged-Navier-Stokes (RANS)-based two-equation turbulence models, was used to simulate cavitation flow inside a cavitating venturi [1]. The reason is that this model may have the possibility of giving the improved prediction performance to the standard k-ε model in the cavitating venturi internal flow where flow separation and reattachment, and re-circulation flow can exist [6].

3.3 Grid System and Boundary Conditions

In this study, unstructured hexahedral grid system generated by ICEM-CFD was used (see Fig. 2). The full geometry of the cavitating venturi was considered in case the flow could not maintain the symmetrical pattern while passing through the diffusion section.

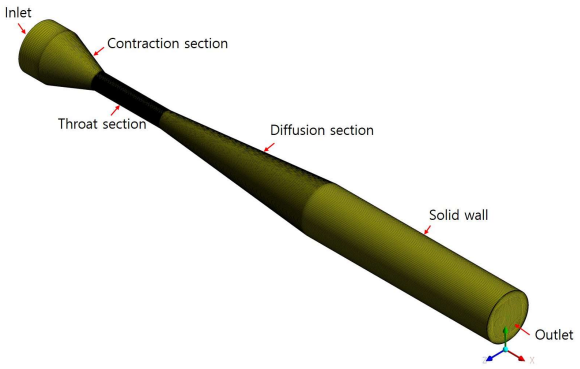

Fig. 2. Grid system.

The total number of grids used in the calculation was in the range of about between 4.5×10^6 and 5.0×10^6 depending on the contraction ratio. To properly predict cavitation flow, dense grid distribution near the solid wall, the contraction and diffusion section, and the straight throat section were used [1].

Inlet condition was the specified constant upstream pressure in the range of between P_{in} = 120 kPa and 350 kPa [1]. Constant turbulent kinetic energy and turbulent dissipation rate was applied [1]. Volume fraction for water vapor was assumed to be 0. Static pressure of 101,325 Pa was specified as an outlet-boundary condition [1]. No-slip condition was applied at the solid wall [1]. To model the flow in the near-wall region, the automatic wall treatment was applied [1].

4. Results and Discussion

Fig. 3 shows the comparison of the static pressure drop (between inlet and outlet) versus inlet velocity depending on the contraction ratio ($\gamma=d/D$). As the magnitude of contraction ratio increased from 0.15 to 0.35, the gradient between static pressure drop and inlet velocity became smaller. The predicted results for γ = 0.25 showed good agreement with the experimental data.

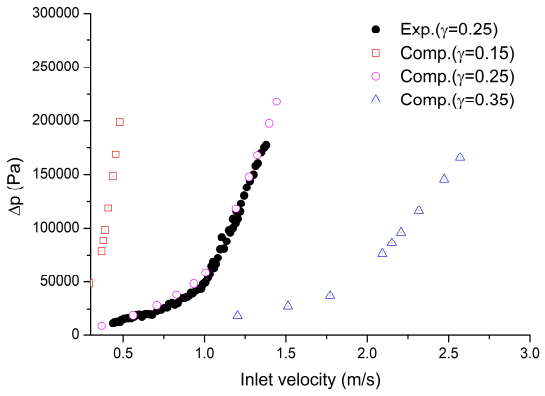

Fig. 3. Static pressure drop versus inlet velocity depending on the contraction ratio.

Fig. 4 shows the distribution of vapor volume fraction at the cross-sections perpendicular to the axial direction. For γ = 0.15, the cavitation flow was hardly seen in the throat region. On the other hand, in cases of γ = 0.25 and 0.35, cavitation flow occurred near the wall of the venturi throat section. As the flow moved toward the entrance of the venturi diffusion section, the cavitation region was enlarged and then it gradually disappeared in the downstream.

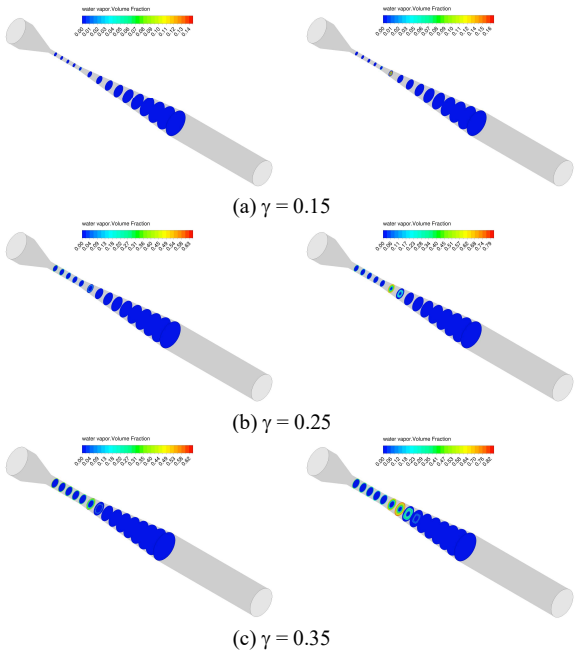

Fig. 4. Distribution of vapor volume fraction at the cross-sections perpendicular to the axial direction (left; P_{in} = 190 kPa, right; P_{in} = 270 kPa).

Fig. 5 shows the massflow average of vapor volume fraction at the cross-sections perpendicular to the axial direction. As the contraction ratio decreased at the corresponding inlet pressure, the peak magnitude of massflow average of vapor volume fraction in both the throat and the diffusion section tended to increase. On the other hand, the decrease in the contraction ratio lead to flow rate reduction as shown in Fig. 3.

5. Conclusions

In this study, simulation of cavitation flow inside a cavitating venturi was conducted with ANSYS CFX R19.1 to investigate the internal flow pattern depending on the contraction ratio for the straight throat section of the cavitating venturi. Main conclusions can be summarized as follows:

(1) While the cavitation flow was hardly seen in the throat region for γ = 0.15, it occurred near the wall of the venturi throat section in case of γ = 0.25 and 0.35. Regardless of the contraction ratio, as the flow moved toward the entrance of the venturi diffusion section, the cavitation region was enlarged and then it gradually disappeared in the downstream.

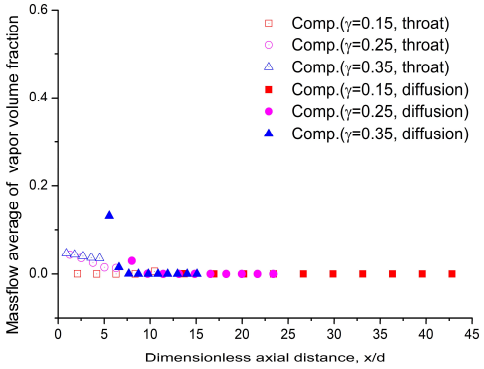

(a) P_{in} = 190 kPa

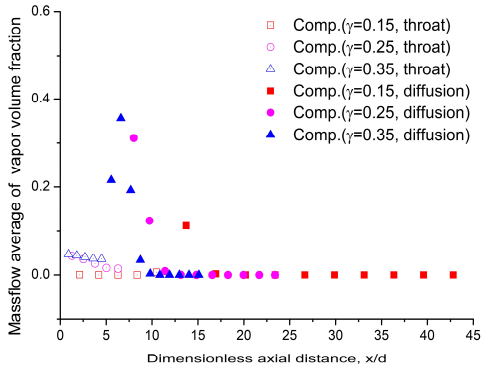

(b) P_{in} = 270 kPa

Fig. 5. Massflow average of vapor volume fraction at the cross-sections perpendicular to the axial direction.

(2) As the contraction ratio decreased at the corresponding inlet pressure, the peak magnitude of massflow average of vapor volume fraction in both the throat and the diffusion section tended to increase. On the other hand, the decrease in the contraction ratio lead to flow rate reduction.

The numerical modeling and calculation results presented in this study may be useful in evaluating the design adequacy of the cavitating venturi, installed in the common line of the auxiliary water supply system in the future.

DISCLAIMER

The opinions expressed in this paper are those of the author and not necessarily those of the Korea Institute of Nuclear Safety (KINS). Any information presented here should not be interpreted as official KINS policy or guidance.

ACKNOWLEGEMENT

This work was supported by the Nuclear Safety Research Program through the Korea Foundation Of Nuclear Safety (KOFONS) using the financial resource granted by the Nuclear Safety and Security Commission (NSSC) of the Republic of Korea (No. 1805007).

REFERENCES

[1] G. H. Lee, J. H. Bae, CFD Simulation of Cavitation Flow inside a Cavitating Venturi using ANSYS CFX, Transactions of the Korean Nuclear Society Virtual Spring Meeting, July 9-10, 2020.
[2] KHNP, Final Safety Analysis Report – Shinkori 3 & 4, 10.4.9. Auxiliary Feedwater System, 2019.
[3] G. H. Lee, J. H. Bae, Investigation of the Internal Flow Pattern depending on Inclination Angle Magnitude in the Convergent Section of the Cavitating Venturi, SAREK Summer Annual Conference, Pyeongchang, June 17-19, 2020.
[4] G. H. Lee, J. H. Bae, A Numerical Study for the Effect of the Magnitude of the Divergent Section Angle on the Cavitating Venturi Internal Flow Pattern, 11st National Congress on Fluids Engineering, Jeju, Korea, August 12-14, 2020.
[5] H. Shi, M. Li, P. Nikrityuk, Q. Liu, Experimental and Numerical Study of Cavitation Flows in Venturi Tubes: From CFD to an Empirical Model, Chemical Engineering Science, Vol.207, p. 672, 2019.
[6] G. H. Lee, Comparative Study for Prediction Accuracy of RANS Turbulence Models: Multi-Phase Flow in the Cavitating Venturi, 7th International Conference on Fluid Flow, Heat and Mass Transfer, Niagara Falls, Canada, November 15-17, 2020.